Measurement of Membrane Potential and $[Ca^{2+}]_i$ in Cell Ensembles: Application to the Study of Glutamate Taste in Mice

Yukako Hayashi,*¶ M. Muz Zviman,* Joseph G. Brand,*§ John H. Teeter,*# and Diego Restrepo*#
*Monell Chemical Senses Center, #Department of Physiology, University of Pennsylvania, and §Veterans Affairs Medical Center, Philadelphia, Pennsylvania 19104 USA, and ¶The Research Institute for Food Science, Kyoto University, Uji, Kyoto 611, Japan

ABSTRACT We have studied the spectral properties of the voltage-sensitive dye, 1-(3-sulfonatopropyl)-4-[β[2-(di-*n*-octylamino)-6-naphtyl]vinyl] pyridinium betaine (di-8-ANEPPS), and the Ca^{2+}-sensitive dye, fura-2, in azolectin liposomes and in isolated taste buds from mouse. We find that the fluorescence excitation spectra of di-8-ANEPPS and fura-2 are largely nonoverlapping, allowing alternate ratio measurements of membrane potential and intracellular calcium ($[Ca^{2+}]_i$). There is a small spillover of di-8-ANEPPS fluorescence at the excitation wavelengths used for fura-2 (340 and 360 nm). However, voltage-induced changes in the fluorescence of di-8-ANEPPS, excited at the fura-2 wavelengths, are small. In addition, di-8-ANEPPS fluorescence is localized to the membrane, whereas fura-2 fluorescence is distributed throughout the cytoplasm. Because of this, the effect of spillover of di-8-ANEPPS fluorescence in the $[Ca^{2+}]_i$ estimate is <1%, under the appropriate conditions. We have applied this method to study of the responses of multiple taste cells within isolated taste buds. We show that membrane potential and $[Ca^{2+}]_i$ can be measured alternately in isolated taste buds from mouse. Stimulation with glutamate and glutamate analogs indicates that taste cells express both metabotropic and ionotropic receptors. The data suggest that the receptors responding to 2-amino-4-phosphonobutyrate (L-AP4), presumably metabotropic L-glutamate receptors, do not mediate excitatory glutamate taste responses.

INTRODUCTION

Taste receptor cells are typically clustered in oval-shaped taste buds embedded in the epithelium of the oral cavity, as well as in the skin of some fishes (Kinnamon and Cummings, 1992; Gilbertson, 1993). Taste buds may contain from 30 to over 150 cells, depending upon the species (Kinnamon, 1987; Reutter and Witt, 1994). Taste cells, which possess voltage-dependent ion channels typical of other excitable cells, detect taste stimuli and relay information on the quality and intensity of the taste stimulus via synaptic connections with afferent nerve fibers. In addition to synaptic connections from taste cells onto afferent nerve fibers, several other types of cell-to-cell interactions have been proposed within taste buds, including electrical coupling, reciprocal synapses between receptor cells and nerve fibers, and release of neuromodulators from some basal cells (Reutter, 1971, 1978; Yang and Roper, 1987; Teeter, 1985; Ewald and Roper, 1995; Delay et al., 1993). Therefore, taste buds may be functional units within which local signal processing takes place. Because of this, we have sought to use optical methods to measure multiple functional parameters in taste cells within isolated taste buds.

Multiparameter optical recording with high spatial and temporal resolution has played a key role in understanding the behavior of multicellular systems (cf. Bright, 1993). With this technique, two or more dyes that differ either in excitation or emission properties are employed to record multiple biological parameters in a preparation. Multiparameter optical recording allows the direct comparison of the response of two or more cellular parameters in single cells and has been applied to numerous systems for simultaneous or alternate measurements of parameters such as pH and $[Ca^{2+}]_i$ (Martinez-Zaguilan et al., 1991; Morris et al., 1994), mitochondrial motility and membrane potential (Loew et al., 1993), or membrane potential and $[Ca^{2+}]_i$ (Ochsner et al., 1991; Kremer et al., 1992; Chacon et al., 1994). Because of the complicated potential interactions between intracellular calcium concentration and membrane potential in excitable cells, the simultaneous measurement of membrane potential and calcium is of particular interest. To our knowledge, the simultaneous measurement of membrane potential and $[Ca^{2+}]_i$ using excitation ratio dyes has only been reported for so-called slow voltage-sensitive dyes (VSDs) (Martinez-Zaguilan et al., 1991; Kremer et al., 1992; Chacon et al., 1994), which cannot be utilized to follow fast changes in membrane potential occurring in excitable cells (see Loew, 1993, for a discussion of "slow" and "fast" VSDs).

In this paper we report a method that uses the calcium-sensitive dye fura-2 (Grynkiewicz et al., 1985) and the fast voltage-sensitive dye di-8-ANEPPS (Bedlack et al., 1992; Loew, 1993; Rohr and Salzberg, 1994) to perform rapid alternate measurement of membrane potential and $[Ca^{2+}]_i$ in cell ensembles. We show that this method is amenable for use with isolated mouse taste buds, and we employ it to determine whether mouse taste cells are responsive to metabotropic and ionotropic glutamate receptor agonists, as suggested by previous molecular biological (Chaudhari et

Received for publication 19 January 1996 and in final form 8 May 1996.
Address reprint requests to Dr. Diego Restrepo, Monell Chemical Senses Center, 3500 Market St., Philadelphia, PA 19104. Tel.: 215-898-6899; Fax: 215-898-2084; E-mail: restrepd@pobox.upenn.edu.

0006-3495/96/08/1057/14 $2.00

al., 1994) and electrophysiological (Teeter et al., 1992) studies.

MATERIALS AND METHODS

Reagents and solutions

The composition of the solutions used in the liposome experiments was (in mM): high Na^+: 140 NaCl, 10 KCl, 10 HEPES (pH 7.2); high K^+: 140 KCl, 10 NaCl, 10 HEPES (pH 7.2). Ringer's solution was (in mM): 145 NaCl, 5 KCl, 1 $CaCl_2$, 1 Na-pyruvate, 20 HEPES (pH 7.2) buffered with NaOH. Di-8-ANEPPS, fura-2, fura-2 acetoxymethyl ester (AM), and pluronic F127 were from Molecular Probes (Eugene, OR). Elastase (no. 4187) and collagenase (no. 2292) were obtained from Worthington Biochemical Corp. (Freehold, NJ). All other reagents were from Sigma (St. Louis, MO).

Liposome preparation

Liposomes were prepared from soybean total phosphatide extract (45% lecithin, 20% phosphatidylethanolemine, 20% phosphatidylserine, 10% inositol-containing phospholipids, and 5% sterols and glycoproteins, purchased from Avanti Polar Lipids (Birmingham, AL). Lipids (12.5 mg) and 0.5 mg cholesterol were dissolved in chloroform (about 0.5 ml) and dried under nitrogen on the walls of a glass vial. One (1) milliliter of the intravesicular solution (either high Na^+ or high K^+) was added, and the vial was placed in a bath sonicator for 15 min. The liposome suspension was then diluted into extravesicular solution in a ratio of 0.2 ml of vesicle suspension to 3 ml of extravesicular solution (either high Na^+ or high K^+). Thus the gradient for K^+_o/K^+_i was 18.6 to 140 mM (high Na^+ out/high K^+ in) and 131.3 to 10 mM (high K^+ out/high Na^+ in), corresponding to Nernst potentials for K^+ of -51 mV and 65 mV.

Fluorescence measurements in liposome suspensions

Di-8-ANEPPS (75 μM final concentration) was added to the intravesicular solution in which the lipids were sonicated. Because the liposome suspension was diluted into the extravesicular solution (0.2 ml into 3 ml), the final concentration of the dye in the cuvette was 5 μM. The liposome suspension was placed in the sample holder of a PTI Deltascan fluorimeter (South Brunswick, NJ), which is capable of exciting at alternate wavelengths. All measurements were performed at room temperature. Two excitation and one emission wavelengths were selected using computer-driven scanning monochromators with slits of 4 nm. Fluorescence emission was quantified by photon counting, and the signal was integrated for 1 s.

Isolation of taste buds

Taste buds were prepared from foliate and vallate papillae of 7–11-week-old glutamate-taster C3H HeJ mice (Ninomya and Funakoshi, 1989) using a procedure modified from Gilbertson et al. (1993). After washing the tongues with oxygenated (O_2/CO_2, 95/5%) divalent cation-free Ringer's solution, extracellular solution containing 2.5 mg/ml collagenase, 2.0 mg/ml elastase, and 18 units/ml DNAse was injected between the epithelium and the muscle. The tongues were incubated in oxygenated divalent cation-free solution at 32°C for 50–65 min. The epithelium was then peeled off from the underlying connective tissue using fine forceps, and was set upside down on a Sylgard-lined dish. Taste buds were sucked from the epithelium with a glass pipette with an opening of approximately 80 μm and plated onto a no. 0 glass coverslip coated with concanavalin A (1 mg/ml). It is important to state that this procedure does not result in the isolation of intact taste buds, but rather of fragments of taste buds (referred to as isolated taste buds in the rest of the manuscript). These isolated taste buds contained anywhere from 5 to 30 taste cells. Because of depth of field limitations, it was not possible to record from all cells in each isolated taste bud.

Isolated buds were loaded with fura-2 by preincubation for 30–60 min in Ringer's solution containing 2 μM fura 2/AM and 20 μg/ml pluronic F127 (Grynkiewicz et al., 1985). At the end of this incubation, the loading solution was replaced by Ringer's containing 5–30 μM VSD di-8-ANEPPS and 80 μg/ml pluronic F127 (Bedlack et al., 1992; Rohr and Salzberg, 1994). After a further 10–15 min incubation, the coverslip was mounted at the bottom of a chamber placed on the stage of a Nikon Diaphot 300 microscope. The taste buds were continuously perfused with Ringer's for 15–30 min before starting the measurements. This wash with dye-free Ringer's solution was important to minimize baseline drift of the fluorescence ratio for di-8-ANEPPS (see below under Results). Measurements were performed at room temperature. Stimuli were delivered by gravity perfusion; complete exchange of solution took place within 5–20 s, depending on the location of the cells on the slide relative to the perfusion inlet.

Fluorescence microscopy with isolated taste buds

Fluorescence measurements in isolated buds were performed with an imaging system from T.I.L.L. Photonics GmbH (Munich, Germany) (Messler et al., 1996). Excitation light was provided by a 75-W xenon lamp. Wavelength selection was attained by the rotation of a diffraction grating mounted on a high-performance optical scanner capable of switching wavelengths in less than 5 ms. A pinhole aperture selected a bandwidth of 12 nm. The excitation light was fed via fiber optics into the epifluorescence port of a Nikon Diaphot 300 microscope equipped with a 515-nm dichroic mirror. The specimen was imaged with a 40× Nikon fluor oil immersion objective with 1.4 n.a. Emitted light passed through a wide barrier filter (525–600 nm) and was imaged with an SC-90-cooled CCD camera from Theta System Elektronik GmbH (Munich, Germany). Each image was integrated over time (100–2000 ms, depending on the intensity of the image) and was digitized with 12 bits of resolution. Image acquisition and analysis were performed under computer control using a modification of img8, a program written in C++, which was kindly provided to us by Dr. Bernd Lindemann. Four images at different excitation wavelengths were typically acquired in each experiment, and the ratio image for either of the two pairs of wavelengths could be displayed during acquisition.

To quantify $[Ca^{2+}]_i$, the specimen was excited alternately at 340 (Ca^{2+}-sensitive) and 360 nm (Ca^{2+}-insensitive) (Grynkiewicz et al., 1985; Restrepo et al., 1995). Individual images were corrected for background fluorescence, and $[Ca^{2+}]_i$ was then estimated in each pixel from the ratio of fluorescence intensity when the specimen was excited at 340 nm divided by fluorescence intensity when excited at 360 nm ($R = F_{340}/F_{360}$), using equation 5 from Grynkiewicz et al. (1985). Calibration procedures for fura-2 were as stated by Restrepo et al. (1995). It is important to indicate that, because of blurring caused by the inclusion of out-of-focus fluorescence in images obtained with a conventional (nonconfocal) microscope, the estimates in changes in $[Ca^{2+}]_i$ and membrane potential in this study will be underestimates of their true values (Bernhardt et al., 1996).

To calculate time courses for $[Ca^{2+}]_i$ and membrane potential for a single cell within an isolated taste bud (as shown, for example, in Fig. 6), rectangular regions of interest were drawn, and the average fluorescence emitted (after subtraction of background) was determined at each excitation wavelength. The regions of interest used for the calculation of $[Ca^{2+}]_i$ were limited to the cytoplasm, and the regions of interest drawn for calculation of voltage were thin rectangular regions within the plane of the membrane. Because neighboring cell membranes are adjacent, measurement of membrane potential in cells located within a cluster was inevitably contaminated by the signal from adjacent cells. Whenever possible, rectangular regions used to determine voltage were drawn in regions where the cell was sticking out of the cluster.

RESULTS

Excitation spectra for di-8-ANEPPS and fura-2 are largely nonoverlapping

The fluorescent dyes fura-2 and di-8-ANEPPS can be employed to determine calcium concentration (fura-2, Grynkiewicz et al., 1985) and membrane potential (di-8-ANEPPS, Bedlack et al., 1992; Loew, 1993; Rohr and Salzberg, 1994) in single cells. Both dyes can be used in ratio mode, where the specimen is alternately excited at two wavelengths, and the fluorescence emission is recorded at a third (longer) wavelength. In ratio mode, the calcium concentration or the membrane voltage can be computed from the ratio (R) of the intensity of the fluorescence emitted when the preparation was excited at the first wavelength (F_1) divided by the fluorescence emitted when the preparation was excited at the second wavelength (F_2).

$$R = (F_1/F_2). \quad (1)$$

Ratio determination of a cellular parameter has the advantage that it corrects for extraneous factors affecting fluorescence intensity of the dye, such as dye leakage, loading inhomogeneity, etc. (see Nuccitelli, 1994, for a review).

The fact that di-8-ANEPPS and fura-2 are excited in the visible (Bedlack et al., 1992) and ultraviolet (Grynkiewicz et al., 1985) wavelength ranges, respectively, suggests that it might be possible to use them to simultaneously record voltage and $[Ca^{2+}]_i$ in the same preparation. To confirm this suggestion, we carried out a study of the spectral dependence of excitation and emission of these two dyes (Fig. 1). As shown in the figure, the excitation spectra of the Ca^{2+}-sensitive dye fura-2 and the VSD di-8-ANEPPS are largely nonoverlapping, whereas the emission spectra overlap in the region from 500 to 600 nm, indicating that these dyes are suitable for multiparameter optical recording. The excitation and emission spectra for di-8-ANEPPS were recorded in liposomes because the fluorescence of this dye is largely dependent on the solvent. Di-8-ANEPPS spectra recorded in azolectin liposomes were similar to spectra recorded in octanol (not shown). The separation of the excitation spectra for fura-2 and di-8-ANEPPS, and the fact that the two dyes partition into topologically separate regions of cells (the cytoplasm and the cell membrane, respectively), suggested to us that it might be possible to stain a preparation with both dyes and perform alternate ratio measurements of $[Ca^{2+}]_i$ and voltage by exciting alternately at two ultraviolet wavelengths to excite fura-2 (340 and 360 nm) and at two visible wavelengths to excite di-8-ANEPPS (440 and 505 nm).

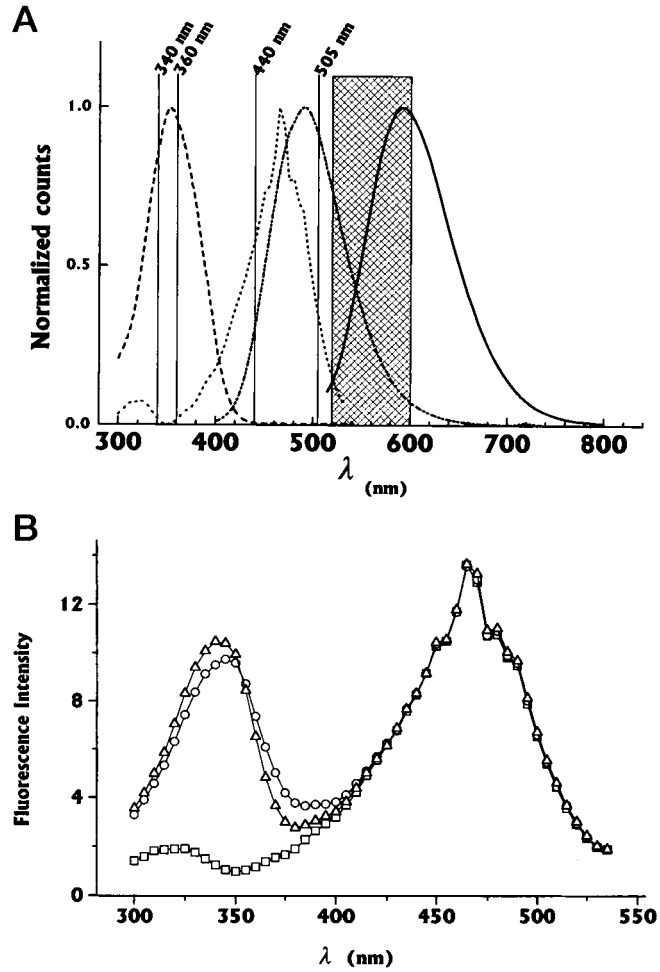

FIGURE 1 The excitation spectra for fura-2 and di-8-ANEPPS are largely nonoverlapping, whereas the emission spectra overlap in the region from 500–600 nm. (*A*) Excitation and emission spectra for fura-2 and di-8-ANEPPS were measured in a suspension of liposomes as detailed in Materials and Methods. – – –, Excitation spectrum for fura-2 recorded at low calcium (1 mM EGTA, no added calcium). Emission was measured at 500 nm. –·–·–, Emission spectrum for fura-2 recorded in the same preparation (excitation wavelength was 360 nm). ·····, Excitation spectrum for di-8-ANEPPS (emission measured at 550 nm). ——, Emission spectrum for di-8-ANEPPS (440 nm excitation). The hatched bar represents the bandwidth of the emission filter used in the measurements of voltage and $[Ca^{2+}]_i$ in isolated taste buds. (*B*) The intensity of the light emitted by di-8-ANEPPS upon excitation at visible wavelegths (440–505 nm) is not modified by changes in fura-2 fluorescence induced by addition of fura-2 to the cuvette, or by a subsequent change in $[Ca^{2+}]$. Excitation spectra were measured in a suspension of di-8-ANEPPS-loaded liposomes with 550 ± 4 nm emission. □, Spectrum before addition of fura-2. △, ○, Spectra after the addition of 2 μM fura-2 in the presence of 300 μM (△) or 400 nM (○) free Ca^{2+}. In all cases fluorescence intensities were arbitrarily normalized.

The voltage dependence of di-8-ANEPPS fluorescence is compatible with both excitation and emission ratio determinations of voltage

In the past, the VSDs di-8- and di-4-ANEPPS have been used in the ratio mode to measure membrane potential in liposomes and single cells (Montana et al., 1989; Bedlack et al., 1992), using excitation wavelengths of 450 and 510 nm. However, in the single cell experiments, the emission bandwidth used was >570 nm, a window that would exclude most of the fura-2 fluorescence. This raised the question of whether it was possible to perform ratio measurements using a wider emission bandwidth that would overlap with

the fura-2 spectrum. To investigate this issue, we incorporated di-8-ANEPPS into azolectin liposomes and recorded the fluorescence properties of the dye at different membrane potentials. Liposome suspensions are a relatively simple model system that has previously been used to study the voltage dependence of VSD (Montana et al., 1989). As in previous work with liposomes (Montana et al., 1989), the membrane potential was manipulated by addition of the K^+ ionophore valinomycin in the presence of different transmembrane potassium gradients, which effectively clamps the membrane potential to the potassium equilibrium potential (E_k).

Fig. 2 *A* shows traces of the fluorescence ratio ($R = F_{440}/F_{505}$) as a function of time, using excitation wavelengths of 440 and 505 nm and recording emission at 550 nm (4 nm bandpass). A 65-mV depolarization elicited by the addition of valinomycin in the presence of an inward transmembrane K^+ gradient caused a 5% increase in the ratio, whereas the addition of valinomycin in the absence of a K^+ gradient caused little change in the ratio, in agreement with previous measurements in a liposome preparation by Montana et al. (1989). Because the voltage dependence of di-8-ANEPPS fluorescence follows a charge-shift electrochromic mechanism (Loew, 1993), the dependence of the voltage sensitivity of fluorescence intensity as a function of excitation and emission wavelengths is not as simple as, for example, the change in excitation properties of fura-2, which follows mass-action laws (Grynkiewicz et al., 1985). Fig. 2 *B* shows the dependence of the percentage change in fluorescence intensity for a 65-mV depolarization of di-8-ANEPPS-loaded liposomes at two different excitation wavelengths as a function of emission wavelength. The magnitude of the change in the ratio is dependent on the choice of both excitation and emission wavelengths, as expected for an electrochromic mechanism.

The voltage dependence of the fluorescence properties of di-8-ANEPPS shown in Fig. 2 *B* is consistent with the measurement of membrane potential employing either the ratio of fluorescence emitted when excited at two wavelengths (excitation ratio) or the ratio of fluorescence intensity using two different emission filters and one excitation wavelength (emission ratio). This is illustrated in Tables 1 and 2, where the changes elicited by a 65-mV depolarization in different excitation and emission ratios have been calculated from the data shown in Fig. 2 *B*. Table 1 shows the change in the excitation ratio for two different emission bandwidths. As expected, the excitation ratio used by Bedlack and co-workers to measure the membrane potential in single cells (Bedlack et al., 1992) (emission >570 nm) increases by 6.4% with a 65-mV depolarization. However, as shown in the table, a bandwidth (>525) that would be suitable for rapid alternate measurements of $[Ca^{2+}]_i$ and voltage, because it overlaps partially with the fura-2 emission spectrum, can also be used to record voltage-dependent changes in the excitation ratio of di-8-ANEPPS. Indeed, use of the wider bandwidth is preferable because a larger amount of the emitted light is collected by the detection system, resulting in lower noise in the measurement.

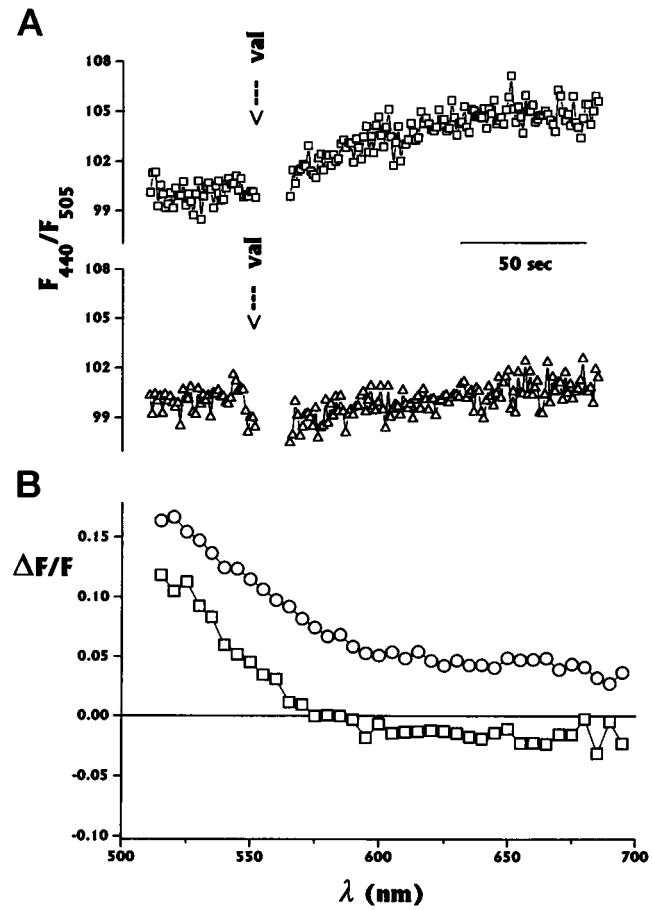

FIGURE 2 Effect of a 65-mV depolarization on the fluorescence emitted by di-8-ANEPPS from a suspension of azolectin liposomes. (*A*). Fluorescence ratio ($R = F_{440}/F_{505}$) as a function of time for liposomes in the presence of different transmembrane potassium gradients (with potassium diffusion potentials of +65 (□) and 0 mV (△). A 65-mV depolarization induced by the addition of valinomycin (50 μM) resulted in a 5% increase in the ratio in this experiment, whereas the addition of valinomycin in the absence of a transmembrane K^+ gradient resulted in a slight transient decrease in the signal. The figure is representative of five independent determinations. The addition of dimethyl sulfoxide, the vehicle used for solubilization of the valinomycin stock, resulted in no change in the ratio (not shown). Excitation wavelengths were 440 and 505 nm, and emission wavelength was 550 nm (4-nm bandwidth). Notice that the addition of valinomycin in the absence of a K^+ gradient did result in a slight transient decrease in the ratio. This phenomenon has been observed by others in a liposome preparation and was attributed to a direct effect of valinomycin on the dye (Montana et al., 1989). This transient effect of valinomycin could also be due to the Donnan equilibrium potential that is likely to exist in a liposome possessing negatively charged lipids on its membrane, and a large surface-to-volume ratio. (*B*) Fractional change in fluorescence ($\delta F/F$) for a 65-mV depolarization as a function of emission wavelength for 440 (○) and 505 (□) nm. This figure is representative of three independent experiments.

The data in Fig. 2 also suggest that it is possible to perform an emission ratio determination of voltage using di-8-ANEPPS. As shown in Table 2, the magnitude of such a ratio increases by 3–5.6% with a 65-mV depolarization,

TABLE 1 Changes in di-8-ANEPPS excitation ratio ($R = F_{440}/F_{505}$) elicited by a 65-mV depolarization in a liposome suspension

Emission bandwidth (nm)	R 0 mV	R +65 mV	$\Delta R/R_0$ (%)	% emitted light collected
>570	2.04	2.17	6.4	50
>525	2.07	2.21	6.5	99

The excitation ratio ($R = F_{440}/F_{505}$) was calculated at 0 and +65 mV, using the data from the experiment shown in Fig. 2 *B*. F_{440} and F_{505} are the fluorescence intensities recorded when the liposome suspension was excited at 440 and 505 nm, respectively. $\Delta R/R_0$ is the percentage change in the ratio elicited by the 65-mV depolarization. The percentage emitted light collected is the percentage light collected within each bandwidth when excited at 440 nm. The percentage light collected with excitation at 505 nm differed from the values at 440 nm by less than 2%.

depending on the combination of excitation and emission bandwidths chosen. This means that with di-8-ANEPPS, it is not only possible to obtain an estimate of potential using a ratio of alternate excitation wavelengths, but it is possible to determine the voltage difference from a ratio determined from simultaneously measured fluorescence intensities with two different filters.

Excitation ratio measurement of membrane potential and $[Ca^{2+}]_i$ in isolated taste buds

Mouse taste cells loaded with 25 μM di-8-ANEPPS respond to K^+/valinomycin-induced depolarization with an increase in the value of the excitation fluorescence ratio (Fig. 3 *A*; excitation wavelengths were 440 and 505 nm, and the emission bandwidth was 525–600 nm). In accordance with published values, the ratio increased by 8–15% with an 85-mV depolarization (Bedlack et al., 1992). The magnitude of the change in the di-8-ANEPPS excitation fluorescence ratio induced by K^+/valinomycin-induced depolarization was also in the range of 8% to 15% in taste buds double labeled with di-8-ANEPPS and fura-2 (Fig. 3 *B*; excitation wavelengths for di-8-ANEPPS were 440 and 505 nm, and those for fura-2 were 340 and 360 nm). In the double-labeled taste buds it was also possible to record a depolarization-induced increase in $[Ca^{2+}]_i$, which was presumably caused by the opening of voltage-dependent Ca^{2+} channels.

Using our fluorescence microscopy recording setup, and with the combination of excitation and emission bandwidths chosen, RMS noise for the di-8-ANEPPS fluorescence ratio was typically 0.2%, and we could reliably measure stimulus-induced changes in the voltage-dye ratio as small as 0.5%, which corresponds to a change of approximately 5 mV (see Figs. 3, 4, and 6). High signal-to-noise ratios are necessary in imaging systems employed to perform optical recording of membrane potential because of the small dynamic range shown by most VSDs (Bedlack et al., 1992; Loew, 1993; Rohr and Salzberg, 1994).

The main advantage of the ratio method versus recording of fluorescence intensity at one wavelength is that, in principle, it makes the measurement independent of factors that change dye intensity in the absence of changes in membrane potential (e.g., dye bleaching, loss of dye from cells, inhomogeneity in dye loading, etc). As expected, ratio measurements were more stable than single wavelength measurements (Fig. 4 *A*), thus extending the time interval that the dye can be used for comparison of the magnitude of changes in membrane potential. However, as shown in Fig. 4 *B*, when measurements were started shortly (0–5 min) after loading the cells with di-8-ANEPPS, the ratio drifted by as much as 30% in 15 min. In some cases the ratio drifted downward, whereas in others the ratio drifted upward (not shown); in all cases, the ratio approached an asymptotic value 15–30 min after the start of the measurement. The drift in the fluorescence ratio was not due to photobleaching, inasmuch as it persisted during intervals when the excitation beam was blocked (not shown). The magnitude of the drift in fluorescence ratio is large, considering the fact that the dynamic range of the dye is approximately 10% for a 100-mV depolarization. The drift was minimized by incubation of the di-8-ANEPPS-loaded cells in Ringer's devoid of dye for 15–30 min after incubation in the dye-loading solution.

The reason for the drift in fluorescence ratio after loading of the taste buds with di-8-ANEPPS is not clear. However, experiments with liposomes suggest that the drift in the value of the ratio may be due to rearrangement of the dye within the bilayer. When azolectin liposomes were loaded with di-8-ANEPPS during sonication of the liposomes, the excitation ratio was stable as a function of time (data not shown). This happened even though the amount of extra-

TABLE 2 Changes in the di-8-ANEPPS emission ratio ($R = F_1/F_2$) elicited by a 65-mV depolarization in a liposome suspension

Excitation wavelength (nm)	Bandwidth for F_1 (nm)	Bandwidth for F_2 (nm)	R 0 mV	R +65 mV	$\Delta R/R_0$ (%)	F_2/F_{tot} (%)	F_1/F_{tot} (%)
505	525–600	>600	0.94	0.97	2.9	47.5	50.5
505	525–575	>625	0.74	0.78	4.8	25.3	34
440	525–600	>600	1.01	1.04	3.5	49.7	49.3
440	525–575	>625	0.83	0.87	5.6	27.1	32.9

The emission ratio ($R = F_1/F_2$) was calculated at 0 and +65 mV, using the data from the experiment in Fig. 2 *B*. F_1 and F_2 are the fluorescence intensities recorded in the two bandwidths indicated in the table in columns 2 and 3. $\Delta R/R_0$ is the percentage change in the ratio elicited by the 65-mV depolarization. F_1/F_{tot} and F_2/F_{tot} are the percentage emitted light collected within the bandwidths corresponding to F_1 and F_2, respectively.

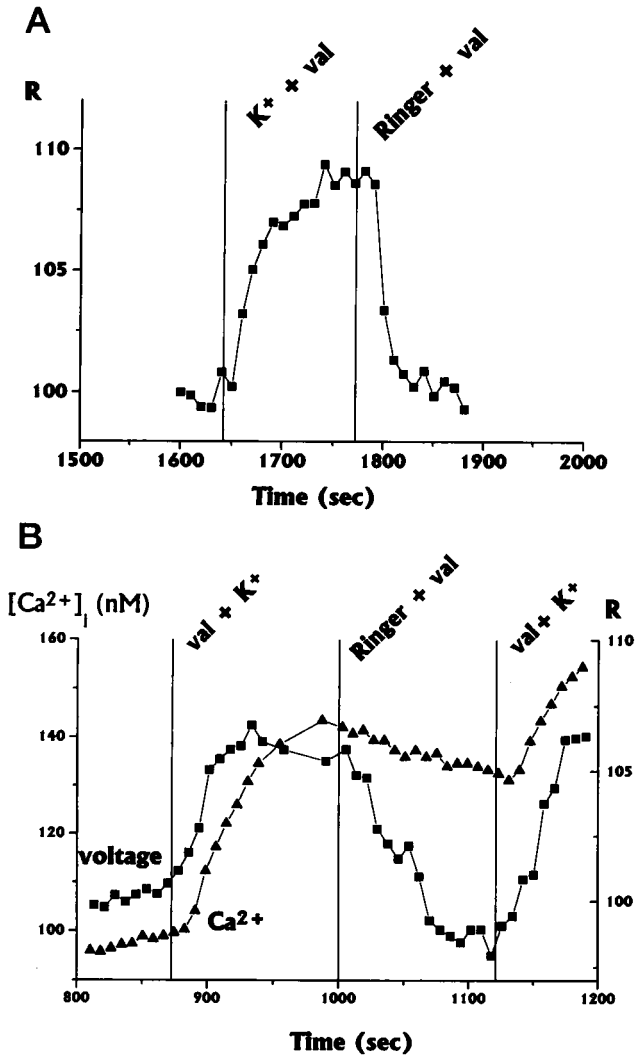

FIGURE 3 Effects of K^+/valinomycin-induced depolarization on measured membrane potential and $[Ca^{2+}]_i$ in taste cells within isolated taste buds. (*A*) Changes in the fluorescence ratio for di-8-ANEPPS ($R = F_{505}/F_{440}$) caused by an 85-mV depolarization in a taste bud that was labeled with the VSD di-8-ANEPPS (no fura-2). Depolarization was induced by replacement of all extracellular Na^+ with K^+ in the presence of the electrogenic K^+ ionophore valinomycin (Montana et al., 1989). (*B*) Effect of K^+/valinomycin-induced depolarization on excitation fluorescence ratio for di-8-ANEPPS (*R*) and in measured $[Ca^{2+}]_i$ in a taste bud double labeled with di-8-ANEPPS and fura-2. □, *R*; △, $[Ca^{2+}]_i$. The di-8-ANEPPS excitation ratio was arbitrarily normalized.

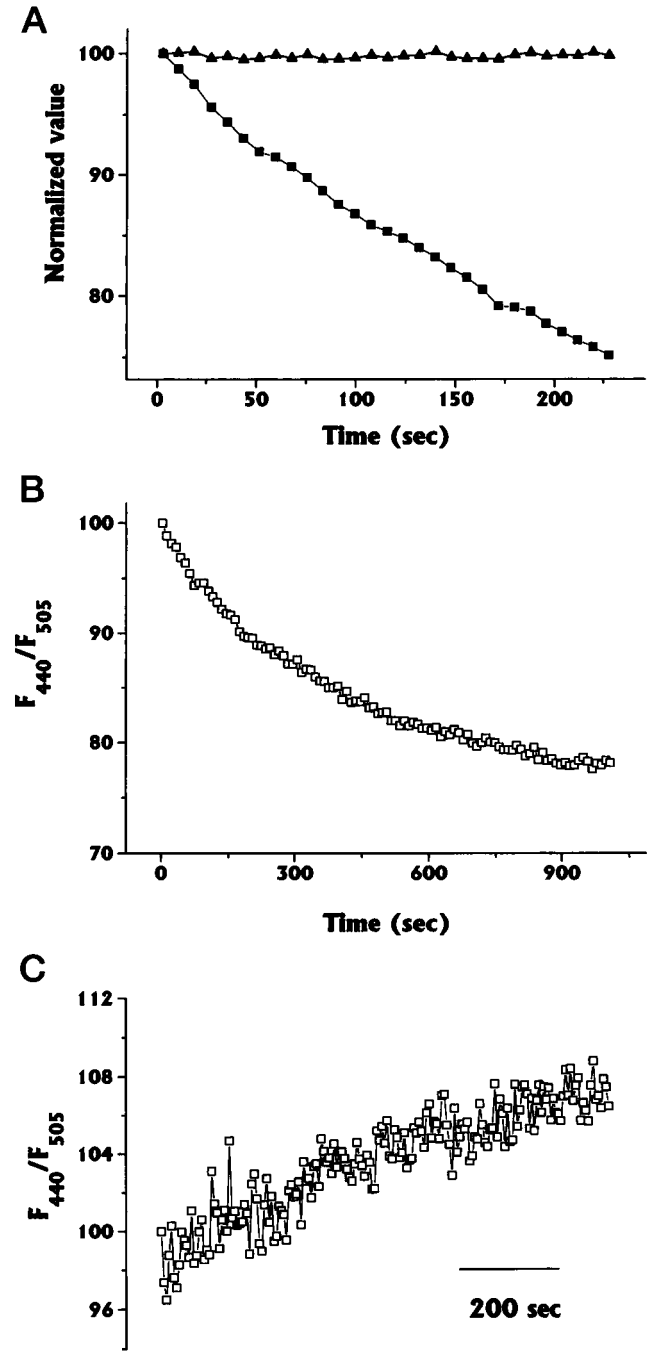

FIGURE 4 Stability of the value of the excitation ratio for di-8-ANEPPS ($R = F_{505}/F_{440}$). (*A*) Fluorescence ratio for the voltage dye di-8-ANEPPS remains stable, even though the individual fluorescence intensities decrease (presumably because of leakage of the dye and/or bleaching). These data were measured in a taste cell in an isolated mouse taste bud loaded with 20 μM di-8-ANEPPS. △, Fluorescence ratio versus time. □, Fluorescence emitted at 440 nm excitation (arbitrary units). (*B*) Measurement of the time course for the fluorescence ratio in a taste cell immediately after loading with di-8-ANEPPS for 15 min. Ratio was arbitrarily normalized to 100 at start of measurement. (*C*) Fluorescence ratio versus time measured in a suspension of liposomes. Di-8-ANEPPS (5 μM) was added directly to the liposome suspension at time 0. In all traces the value of the ratio was arbitrarily normalized to 100 at $t = 0$.

cellular di-8-ANEPPS was diluted by 15-fold at the start of the measurement. However, when the liposomes were loaded by addition of the dye to a suspension of preformed liposomes, the ratio drifted in a manner similar to that of taste buds loaded with di-8-ANEPPS (Fig. 4 *C*). This suggested that the drift in the fluorescence ratio may have something to do with rearrangement of the dye within the lipid bilayer, a concept that is not unreasonable, considering that the fluorescence properties of styryl dyes are greatly dependent on the nature of the bilayer.

Alternate estimation of $[Ca^{2+}]_i$ and membrane potential in isolated mouse taste buds: responses to L-glutamate and glutamate analogs

Experiments with bilayers into which epithelial membrane vesicles derived from vallate taste papillae of mice have been incorporated suggest that this tissue has cation channels that are directly, specifically, and reversibly activated by millimolar concentrations of L-glutamate (Teeter et al., 1992). The L-glutamate-activated conductance is concentration dependent, somewhat selective for Na^+ over K^+ ions, and markedly enhanced by the addition of 5′-GMP at concentrations that alone have no effect on bilayer conductance. These experiments suggest that taste receptors for L-glutamate may be L-glutamate-gated cation channels. However, recent molecular biological and behavioral evidence from rat suggests that L-glutamate taste transduction is mediated by a metabotropic receptor displaying high sequence homology with a metabotropic L-glutamate receptor from brain named mGluR4 (Chaudhari et al., 1994). Nevertheless, little is known about the response of intact taste buds or isolated taste cells to L-glutamate.

To determine whether compounds known to stimulate ionotropic and metabotropic L-glutamate receptors in central nervous neurons stimulate taste cells, we measured $[Ca^{2+}]_i$ and membrane potential in isolated mouse taste buds. We isolated taste buds from foliate and vallate papillae from a glutamate-taster strain of mouse (C3H HeJ) (Ninomya and Funakoshi, 1989), using a modification of

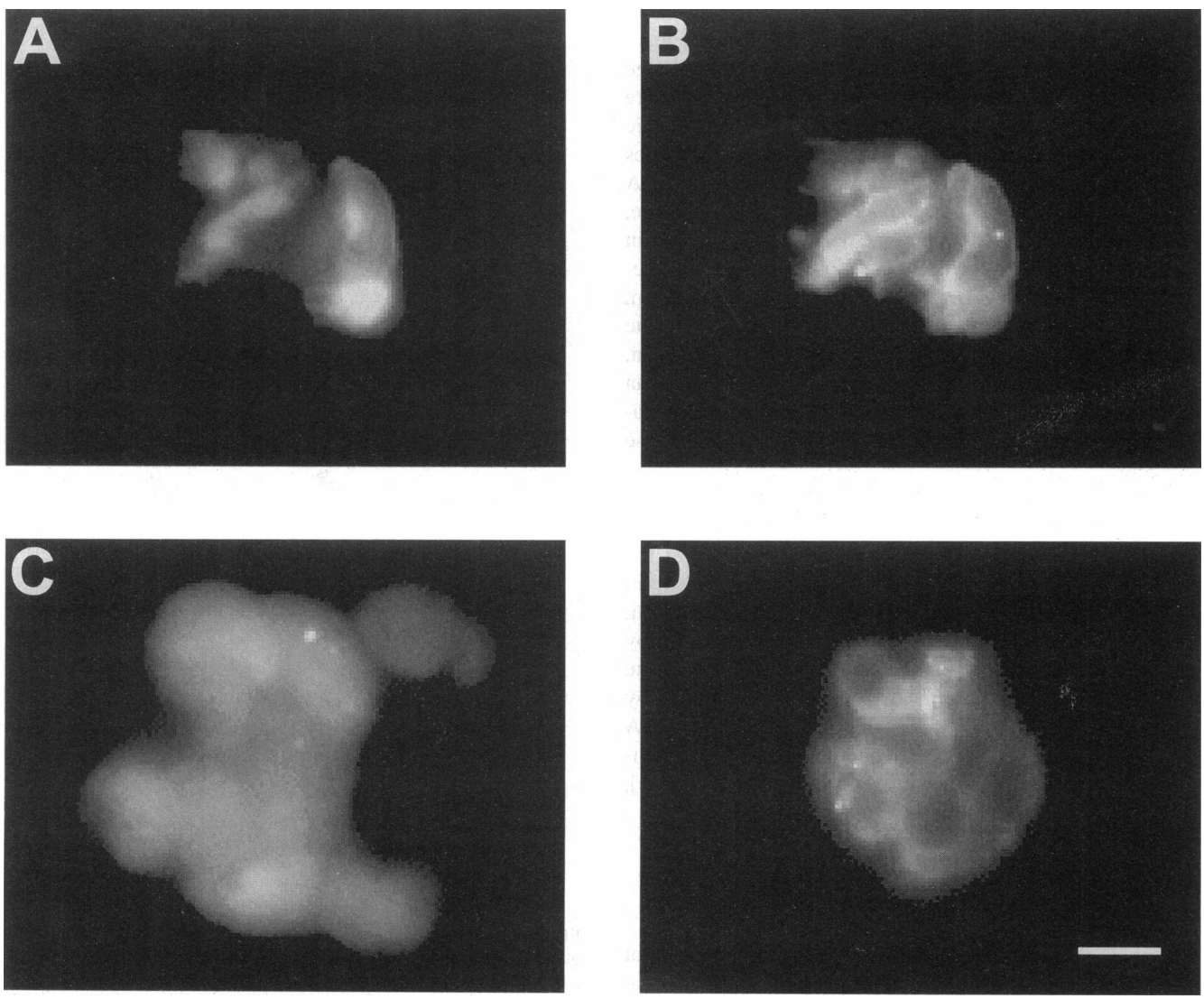

FIGURE 5 Images showing fluorescence emitted by mouse isolated taste buds loaded with fura-2 and di-8-ANEPPS (*A* and *B*), fura-2 only (*C*), or di-8-ANEPPS only. (*A* and *B*) Gray-scale images of an isolated mouse taste bud displaying fluorescence emitted by fura-2 (*A*) (360-nm excitation) and di-8-ANEPPS (*B*) (440-nm excitation). The location of the apical end of the taste bud is indicated with an arrow. (*C*) Gray-scale image of an isolated taste bud loaded with fura-2 only. The excitation wavelength was 360 nm. (*D*) Image of an isolated taste bud loaded with di-8-ANEPPS. The excitation wavelength was 440 nm. The scale bar shown is 10 μm long.

the method of Gilbertson et al. (1993). We loaded all isolated taste buds (n = 23) with fura-2, and double-loaded 16 of 23 taste buds with fura-2 and di-8-ANEPPS for alternate determination of $[Ca^{2+}]_i$ and membrane potential. Fig. 5 shows gray-scale images of the fluorescence emitted by an isolated taste bud when excited at 360 nm (fura-2 fluorescence; 5A) and 440 nm (di-8-ANEPPS fluorescence; Fig. 5 *B*). As expected from the known properties of these dyes, the fluorescence from the Ca^{2+}-sensitive dye is distributed throughout the cytoplasm of the cells, whereas the fluorescence from the VSD is localized mainly to the cell membranes.

In measurements from 23 isolated taste buds, we recorded changes in $[Ca^{2+}]_i$ elicited by 1 mM L-glutamate and glutamate analogs (2-amino-4-phosphonobutyrate, L-AP4, and *N*-methyl-D-aspartate, NMDA) in 55 of 134 taste cells (15 of 23 taste buds; see Fig. 6 for representative records). Responses to L-glutamate and analogs could be elicited more than once, but subsequent responses were smaller. The decrease in the magnitude of the response was not due to toxicity from the voltage dye, because it occurred regardless of whether the cells were loaded with the voltage dye. Interestingly, the metabotropic glutamate receptor agonist L-AP4 primarily elicited decreases in $[Ca^{2+}]_i$, whereas the ionotropic glutamate agonist NMDA elicited increases in $[Ca^{2+}]_i$ (Table 3). In contrast, L-glutamate, which stimulates both ionotropic and metabotropic receptors in the central nervous system, elicited both increases and decreases in $[Ca^{2+}]_i$ in different cells (Table 3). In addition, simultaneous stimulation with L-glutamate and the glutamate taste enhancer 5′GMP (1 mM) (Cagan, 1980; Yamaguchi, 1967) resulted primarily in increases in $[Ca^{2+}]_i$. These data suggest that stimulation of ionotropic or metabotropic glutamate receptors elicits opposite changes in $[Ca^{2+}]_i$ in mouse taste cells.

We performed alternate measurement of membrane potential and $[Ca^{2+}]_i$ in 16 taste buds double labeled with fura-2 and the VSD di-8-ANEPPS. Measurements in the double-labeled taste cells indicated that the increases in $[Ca^{2+}]_i$ occurred simultaneously with cell depolarization, whereas the decreases in $[Ca^{2+}]_i$ were not accompanied by measurable changes in membrane potential (except in one case in which the decrease in $[Ca^{2+}]_i$ was accompanied by depolarization; see Table 4). In addition, L-AP4 and NMDA elicited in some cells a depolarization that was not accompanied by a measurable change in intracellular $[Ca^{2+}]_i$ (Table 4).

Spillover of di-8-ANEPPS fluorescence into ultraviolet excitation wavelengths

As shown in Fig. 1 *A*, changes in fura-2 fluorescence do not alter the di-8-ANEPPS excitation spectrum (measured at wavelengths of >430 nm). In contrast, the excitation spectrum for di-8-ANEPPS does overlap with the excitation spectrum for fura-2 in the ultraviolet region (Fig. 1 *A*). Because of this, measurements of fura-2 fluorescence excited at 340 and 360 nm will include a small amount of

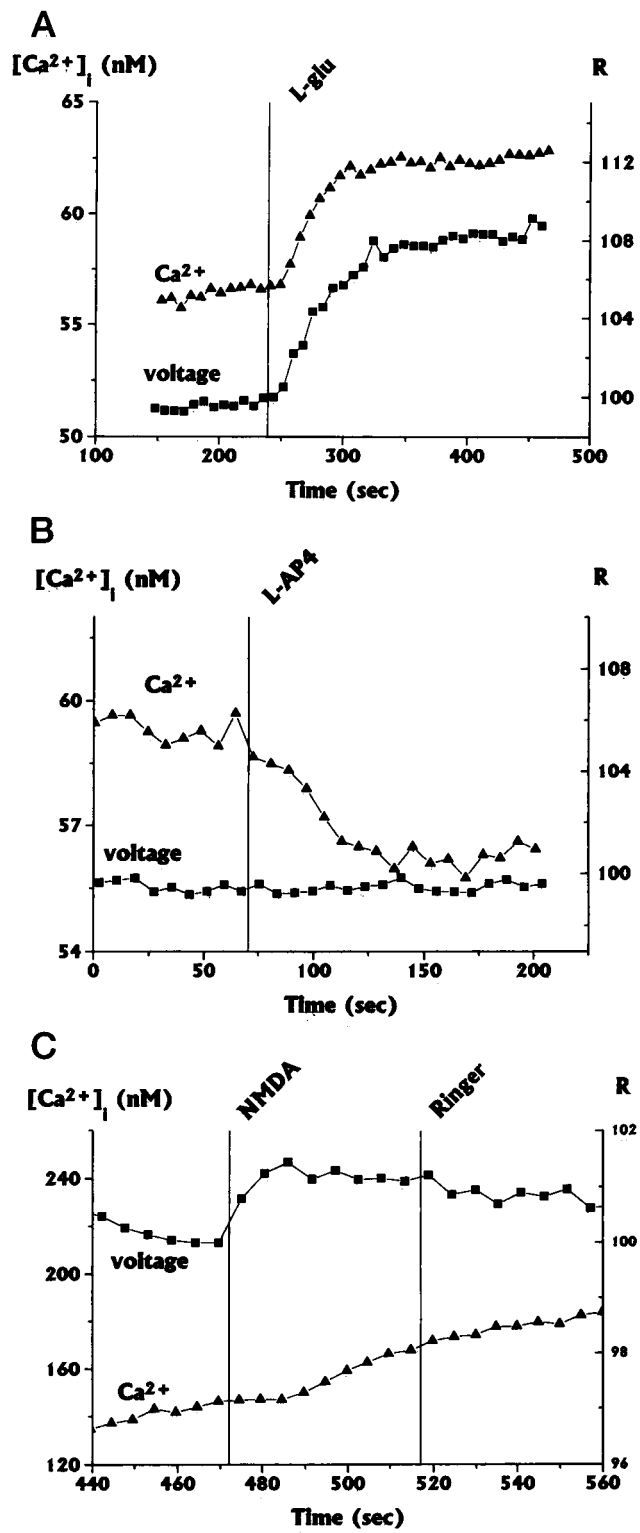

FIGURE 6 Responses of taste cells within isolated mouse taste buds to glutamate and analogs. The stimuli were 1 mM L-Glu (*A*), 1 mM L-AP4 (*B*), and 1 mM NMDA (*C*). The triangles represent the calculated $[Ca^{2+}]_i$ in nM (left axis). The squares are values for the fluorescence ratio ($R = F_{505}/F_{440}$) for the voltage dye di-8-ANEPPS (right axis, arbitrarily normalized to 100 at the time of addition of the stimulus). The vertical line indicates the time of switching of solutions (the stimulus reaches the cell with a delay of 5–20 s).

TABLE 3 Changes in $[Ca^{2+}]_i$ elicited by the addition of glutamate and glutamate analogs

Stimulus	No. of cells responding with increased $[Ca^{2+}]_i$	No. of cells responding with decreased $[Ca^{2+}]_i$	Total no. of cells tested
L-Glutamate	18	7	85
L-AP4	2	12	134
NMDA	8	0	129
L-Glutamate + 5′ GMP	28	3	116

Results are from 23 isolated taste buds loaded with fura-2 or fura-2 and di-8-ANEPPS.

fluorescence emitted by di-8-ANEPPS. It is therefore important to estimate the effect of changes in di-8-ANEPPS fluorescence on fura-2 estimates of $[Ca^{2+}]_i$.

Table 5 shows for a liposome suspension the amount of spillover of di-8-ANEPPS fluorescence into the ultraviolet (at 340 or 360 nm) expressed as a percentage of the emitted light intensity when di-8-ANEPPS is excited at 440 nm. As shown, the emitted light intensity in the ultraviolet is approximately 10% of the light emitted when excited at 440 nm. More importantly, there is little change in this ratio when the membrane potential is increased by 65 mV (Table 5 and Fig. 7). Therefore, in principle, in a double-label experiment, it should be possible to subtract the spillover of di-8-ANEPPS fluorescence into the ultraviolet, calculated as a percentage of the fluorescence intensity measured when the preparation is excited at 440 nm. However, in the isolated taste bud preparation it is not possible to use this approach, because for taste buds loaded with di-8-ANEPPS only, there is considerable cell-to-cell variation in the ratio of fluorescence emitted when the preparation is excited at 340 or 360 nm to fluorescence emitted when the preparation is excited at 440 nm (Table 6). The variation from cell to cell is not surprising because the spectral properties of styryl dyes are affected by membrane composition, which is likely to vary from cell to cell.

Because of this, we have chosen to perform double-label measurements of $[Ca^{2+}]_i$ and membrane potential under conditions in which this spillover correction is not necessary. This was attained by loading cells with relative amounts of fura-2 and di-8-ANEPPS, which resulted in a ratio of di-8-ANEPPS fluorescence to fura-2 florescence that is low enough not to interfere with the fura-2 measurements. In the following section, we present an empirical parameter (the ratio of F_{360}/F_{440}) that can be used to determine the magnitude of the spillover error. We have used this parameter to ensure that our double-label measurements were performed under conditions that ensure minimal errors in the estimation of $[Ca^{2+}]_i$.

TABLE 4 Depolarization induced by glutamate and analogues in mouse taste cells

Stimulus	Cells responding with a depolarization and an increase in $[Ca^{2+}]_i$	Cells responding with a depolarization and a decrease in $[Ca^{2+}]_i$	Cells responding with a depolarization (regardless of changes in $[Ca^{2+}]_i$)
L-Glutamate	18 (n = 18)	0 (7)	18 (82)
L-AP4	2 (2)	1 (6)	16 (82)
NMDA	5 (6)	0 (0)	14 (77)
L-Glutamate + 5′ GMP	0 (3)	0 (3)	4 (67)

These results were measured in taste buds double labeled with fura-2 and di-8-ANEPPS. L-Glutamate and analogs did not elicit measurable hyperpolarizations in mouse taste cells.

TABLE 5 Spillover of di-8-ANEPPS fluorescence into ultraviolet excitation wavelengths estimated from spectral measurements in a liposome suspension

Membrane potential (mV)	$F_{di8,340}/F_{di8,440}$ (%)	$F_{di8,360}/F_{di8,440}$ (%)
0	11.6 ± 0.2	10.6 ± 0.2
65	11.9 ± 0.4	11.0 ± 0.3

These values were estimated from measurements of the excitation spectrum of di-8-ANEPPS in a suspension of azolectin liposomes at 0 and +65 mV (emission wavelength 560 nm). Values shown are average ± SEM (n = 3). Membrane potential was set using valinomycin and K^+ gradients as stated in Materials and Methods. $F_{di8,x}$ is the fluorescence emitted by di-8-ANEPPS at 560 nm, when excited at x nm.

Quantification of the effect of di-8-ANEPPS fluorescence spillover on fura-2 estimates of $[Ca^{2+}]_i$

Because the spectral properties of di-8-ANEPPS fluorescence are known, it is possible to determine the magnitude

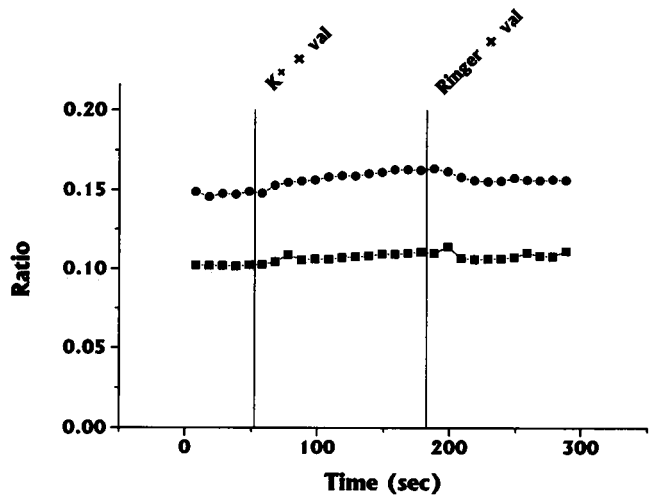

FIGURE 7 Spillover of di-8-ANEPPS fluorescence into ultraviolet: effect of membrane potential measured in a taste cell. Ratio of fluorescence emitted by di-8-ANEPPS at excitation wavelengths of 340 (■) or 360 nm (●) divided by the fluorescence emitted with an excitation wavelength of 440 nm measured in an isolated taste bud loaded with di-8-ANEPPS only. At the time indicated by the line, the membrane potential was depolarized from −85 mV to 0 mV by the addition of K^+ in the presence of valinomycin. Fluorescence intensity was not corrected for differential absorption by filters and lenses at the different wavelengths.

TABLE 6 Spillover of di-8-ANEPPS fluorescence into ultraviolet excitation wavelengths estimated from spectral measurements in isolated taste buds

Statistic	$F_{di8,340}/F_{di8,440}$ (%)	$F_{di8,360}/F_{di8,440}$ (%)
Mean ± SEM	10.9 ± 0.9	15.7 ± 1.2
Maximum value	16.4	21.6
Minimum value	6.1	9.0

These values were estimated from measurements of the excitation spectrum of di-8-ANEPPS in taste cells within isolated taste buds loaded only with di-8-ANEPPS (n = 15 cells from three taste buds). Measurements were performed at resting membrane potential. $F_{di8,x}$ is the fluorescence emitted by di-8-ANEPPS at 525–600 nm, when excited at x nm. Fluorescence intensity estimates were not corrected for differential absorption by filters and lenses at the different wavelengths.

of the error introduced by spillover of di-8-ANEPPS fluorescence in the ultraviolet in the estimates of $[Ca^{2+}]_i$ as follows.

The measured ratio of fluorescence at 340 nm divided by fluorescence at 360 nm (R_{meas}) will include contributions from fura-2 ($F_{f2,340}$ and $F_{f2,360}$) and di-8-ANEPPS ($F_{di8,340}$ and $F_{di8,360}$) fluorescence:

$$R_{meas} = \frac{(F_{f2,340} + F_{di8,340})}{(F_{f2,360} + F_{di8,360})}. \quad (2)$$

Similarly, the estimate of the calcium concentration ($[Ca^{2+}]$) is given by equation 5 of Grynkiewicz et al. (1985):

$$[Ca^{2+}] = K_d(S_{f2}/S_{b2})\frac{(R_{meas} - R_{min})}{(R_{max} - R_{meas})}, \quad (3)$$

where K_d is the apparent dissociation constant for Ca^{2+}; R_{max} and R_{min} are the maximum and minimum values for R_{meas}, respectively; and (S_{f2}/S_{b2}) is the ratio of fluorescence intensity at the second wavelength of excitation (360 nm) for Ca^{2+}-free fura-2 divided by the intensity of fluorescence for Ca^{2+}-bound fura-2.

As shown in Table 5, the intensity of fluorescence contributed by di-8-ANEPPS at 340 nm is approximately equal to the fluorescence contributed at 360 nm (roughly 10% of the fluorescence emitted by di-8-ANEPPS at 440 nm). Therefore, as the amount of di-8-ANEPPS is increased, the denominator and numerator in Eq. 2 increase by roughly the same amount and R_{meas} approaches a value of 1. Consequently, as the amount of di-8-ANEPPS relative to fura-2 increases, $[Ca^{2+}]$ values corresponding to R_{meas} values less than 1 will increase, whereas $[Ca^{2+}]_i$ values corresponding to R_{meas} values higher than 1 will decrease. This is shown in Fig. 8 *A*, where the percentage error in the calculated $[Ca^{2+}]$ is shown as a function of the ratio of fluorescence at 360 nm divided by the fluorescence at 440 nm, an experimental measure of the relative amounts of fura-2 and di-8-ANEPPS. As shown in the figure, the error is relatively minor (<5%), provided that the calcium concentration is not far from the K_d for fura-2 (30 nM < $[Ca^{2+}]$ < 1000 nM), and that the amount of di-8-ANEPPS is not large (F_{360}/F_{440} > 10). The details of the calculation performed to determine the data for Fig. 8 *A* are given in the Appendix.

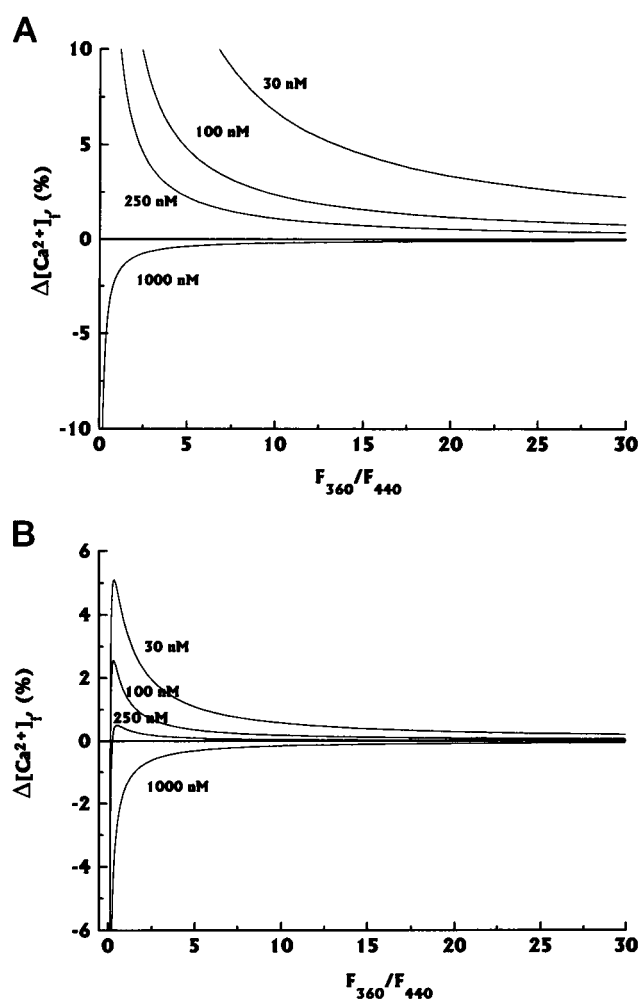

FIGURE 8 Effect of spillover of di-8-ANEPPS fluorescence at ultraviolet excitation wavelengths on $[Ca^{2+}]$ estimates. (*A*) Percentage change in the calculated $[Ca^{2+}]$ ($\Delta[Ca^{2+}]_i$) as a function of the ratio of fluorescence emitted by the cells when excited at 360 nm divided by fluorescence emitted when excited at 440 nm (F_{360}/F_{440}). (*B*) Artifactual percentage change in $[Ca^{2+}]$-induced change in the spillover of di-8-ANEPPS fluorescence upon a 50-mV depolarization ($\Delta[Ca^{2+}]_i$) as a function of the F_{360}/F_{440} ratio. Data for *A* and *B* were calculated as stated in the Appendix for different calcium concentrations shown in the figure.

A more worrisome effect of spillover of di-8-ANEPPS fluorescence into the ultraviolet is that a change in the membrane potential could give rise to an artifactual change in the measured $[Ca^{2+}]$. Fig. 8 *B* shows the magnitude of the change in $[Ca^{2+}]$ for a 65-mV depolarization (details of the calculation are given in Appendix 1). The spillover from di-8-ANEPPS can cause either a decrease or an increase in $[Ca^{2+}]$, depending on the initial $[Ca^{2+}]$ and the relative amounts of fura-2 to di-8-ANEPPS (quantified by the fluorescence ratio F_{360}/F_{440}). However, the error is relatively minor (<1%), provided again that the amount of di-8-ANEPPS is not large (F_{360}/F_{440} > 10).

Therefore, the changes in measured $[Ca^{2+}]$ elicited by spillover of di-8-ANEPPS fluorescence into the ultraviolet are relatively minor. In fact, we were able to detect these effects only in cells that loaded inefficiently with fura-2 (as evidenced by a fura-2/di-8-ANEPPS fluorescence ratio F_{360}/F_{440} of 0.15). In these cells, an 85-mV depolarization induced by the addition of valinomycin in the presence of 150 mM KCl elicited an artifactual decrease in $[Ca^{2+}]_i$ from 107 nM to 97 nM (not shown). All other dual measurements of membrane potential and $[Ca^{2+}]_i$ were performed using fura-2/di-8-ANEPPS fluorescence ratios (F_{360}/F_{440}) of 10–70. Under these conditions, the spillover error is expected to be relatively minor and cannot account for the $[Ca^{2+}]$ changes recorded. These high F_{360}/F_{440} ratios for the $[Ca^{2+}]_i$ measurements were attained by loading the cells with concentrations of fura-2/AM into di-8-ANEPPS, which resulted in fluorescence emission by fura-2 at 360 nm that was about three- to fivefold higher than the fluorescence emission from di-8-ANEPPS at 440 nm in the whole taste bud, and by choosing windows for the calculation of the fura-2 ratio that excluded di-8-ANEPPS fluorescence. This was easily attained, because di-8-ANEPPS fluorescence was localized to the plasma membrane, whereas fura-2 fluorescence was evenly distributed throughout the cytoplasm (Fig. 5).

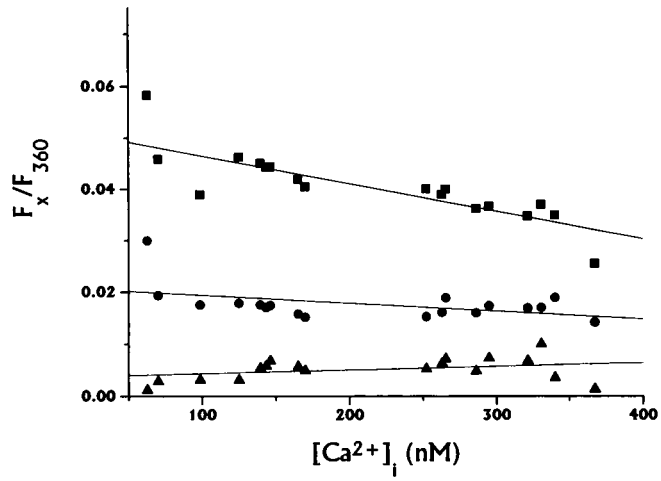

FIGURE 9 Spillover of fura-2 fluorescence into visible excitation wavelengths. The figure shows the dependence of fluorescence emitted by taste cells loaded with fura-2 at excitation wavelengths of 440 (■), 450 (●), and 505 (▲) nm. Fluorescence emitted at wavelength x (F_x) was normalized by dividing by fluorescence emitted at the isosbestic point for fura-2 (F_{360}). Isolated taste buds were loaded with fura-2 (no di-8-ANEPPS) by preincubation in fura-2/AM as detailed in Materials and Methods. Some of the cells were treated with ionomycin to widen the range of $[Ca^{2+}]_i$ studied.

Spillover of fura-2 fluorescence into visible excitation wavelengths

Although the excitation spectrum for fura-2 does not extend into the visible wavelength range (>440 nm; see Fig. 1), cells loaded with fura-2/AM might produce fluorescent by-products or intermediates that fluoresce when excited at visible wavelengths. Because of this possibility, and because even small changes in fluorescence might influence the measurement of membrane potential with di-8-ANEPPS, we determined the fluorescence emitted by taste cells loaded with fura-2 by preincubation with fura-2/AM. Fig. 9 shows the fluorescence emitted by these cells at different wavelengths (440, 450, and 505 nm) relative to fluorescence emitted at the isosbestic wavelength for fura-2 (360 nm). As shown, even though the amount of fluorescence emitted is small relative to the fluorescence emitted when the preparation is excited at 360 nm, the intensity is larger that expected from measurements of fura-2 fluorescence in solution (Fig. 1). The amount of fluorescence emitted by fura-2/AM-loaded cells when the preparation is excited at these visible wavelengths is larger than the amount of autofluoresence measured in taste cells not loaded with fura-2 (not shown), suggesting that a by-product of fura-2/AM hydrolysis emits light when the cells are excited at wavelengths of >440 nm.

In principle, if the fluorescence emitted by these by-products of fura-2/AM hydrolysis changes with $[Ca^{2+}]_i$, they could give rise to an artificial change in the membrane potential measured by di-8-ANEPPS. However, the fluorescence emitted at visible excitation wavelengths by these by products is unlikely to elicit an artifactual change in the measured membrane potential, because the intensity of the light emitted upon excitation at 440–505 nm is a small percentage of the fluorescence emitted by the cells at 360 nm and, more importantly, because the fluorescence emitted is only slightly dependent on $[Ca^{2+}]_i$ at excitation wavelengths between 440 and 505 nm (Fig. 9). Indeed, if an artifactual change in membrane potential had occurred during an increase in $[Ca^{2+}]_i$, its direction would be in the hyperpolarizing direction (because F_{440}/F_{360} decreases as $[Ca^{2+}]_i$ is increased; see Fig. 9), and this was never observed in our experiments (Table 4 and Figs. 3 *B* and 6).

DISCUSSION

Determination of membrane potential and $[Ca^{2+}]_i$ by double labeling with di-8-ANEPPS and fura-2

To determine membrane potential and $[Ca^{2+}]_i$ in the same cell using fluorescent dyes, it is necessary to show that measured changes in fluorescence emitted by one dye are independent of changes in the fluorescence emitted by the other dye. The choice of fura-2 and di-8-ANEPPS provides a nearly ideal situation. Fig. 1 shows that fura-2 does not emit significant fluorescence when excited at wavelengths of >430 nm, and that the fluorescence emitted by di-8-ANEPPS when excited at ultraviolet wavelengths is much smaller than the intensity of fluorescence when di-8-ANEPPS is excited in the visible wavelength range.

Because even a small spillover of fura-2 fluorescence at excitation wavelengths used to excite di-8-ANEPPS (440–505 nm) could cause artifactual changes in measured membrane potential, we determined the characteristics of light emitted by fura-2/AM-loaded taste cells. We found that, as shown in Fig. 9, fura-2/AM-loaded taste cells emitted little fluorescence when excited at wavelengths above 440 nm. More importantly, the data in Fig. 9 show that the effect of an increase in $[Ca^{2+}]_i$ would be to elicit an artifactual decrease in the membrane potential, a situation that was never observed in our studies (see Results). If it is suspected that spillover of fura-2 fluorescence is causing artifactual changes in membrane potential in other cell systems, a better choice of wavelengths would be 450 and 505 nm, because at these two wavelengths there is little change in fluorescence emitted by fura-2-loaded cells as a function of $[Ca^{2+}]_i$ (Fig. 9).

On the other hand, the excitation spectrum of di-8-ANEPPS does overlap slightly with the excitation spectrum of fura-2 (Fig. 1). However, the effect of this spillover can be made relatively small because fura-2 fluorescence and di-8-ANEPPS fluorescence are spatially restricted to the cytoplasm and the plasma membrane, respectively. Because of this, it is possible to use separate windows for the estimation of membrane potential and $[Ca^{2+}]_i$. In fact, even in relatively small cells such as the taste cells used in this study, it was possible to choose windows for analysis where a large percentage of the fluorescence recorded was emitted by fura-2 (and vice versa). This fact, and the fact that the quantum efficiency for di-8-ANEPPS fluorescence in the ultraviolet is relatively low (approximately 10% of the quantum efficiency at 440 nm) ensured that the magnitude of errors induced by the spillover of di-8-ANEPPS fluorescence in estimated values of $[Ca^{2+}]_i$ was relatively small (Fig. 8).

Our calculations provide a procedure to determine whether significant spillover of di-8-ANEPPS fluorescence occurs in a given measurement. It is necessary to ensure that the ratio of fluorescence emitted by the cells when excited at 360 nm divided by fluorescence emitted when excited at 440 nm (F_{360}/F_{440}) be larger than 10 in the analysis window used for the estimation of $[Ca^{2+}]_i$. If the F_{360}/F_{440} ratio, which is an empirical measure of the relative concentrations of fura-2 and di-8-ANEPPS, is lower than 10, it is necessary to take measures to increase the ratio. This can be done by increasing the concentration of fura-2 in the cells or by choosing analysis windows that better exclude di-8-ANEPPS fluorescence. For example, a change in the dichroic mirror would allow the measurement of fura-2 fluorescence using an emission bandwidth from 440 nm to 525 nm, while using an emission bandwidth of >550 nm for di-8-ANEPPS. With these settings, there would be minimal overlap of the fura-2 and di-8-ANEPPS signals (Fig. 1). In addition, for small cells in which blurring of di-8-ANEPPS fluorescence results in the inclusion of di-8-ANEPPS fluorescence in measurements within the cytoplasm, use of deblurring algorithms could improve the F_{360}/F_{440} ratio (Monck et al., 1992; Bernhardt et al., 1996). As a result, deblurring might permit the measurement of $[Ca^{2+}]_i$ closer to the membrane, which is the region of the cell in which changes in $[Ca^{2+}]_i$ associated with neurotransmitter release are expected to take place (Llinas et al., 1992).

Correction for spillover of di-8-ANEPPS fluorescence into fura-2 excitation wavelengths

In principle, it should be possible to perform a double-label experiment regardless of the relative loading of fura-2 and di-8-ANEPPS by correcting for the amount of spillover of di-8-ANEPPS fluorescence into the ultraviolet. We could not perform this correction with the isolated taste bud preparation because in taste cells the amount of spillover into the ultraviolet varied substantially from cell to cell (compare the maximum and minimum values in Table 6). This variation is not surprising, because the spectral properties of styryl dyes are strongly dependent on the lipid composition of the plasma membrane. In more homogeneous cell populations (i.e., in clonal cell lines), the amount of spillover of di-8-ANEPPS fluorescence into the ultraviolet may vary less significantly from cell to cell. In those cases it should be possible to subtract the spillover of di-8-ANEPPS fluorescence from the fura-2 images.

Limitations on speed of acquisition

Although the measurements performed in this study are relatively slow, the method has the potential of being used to study events in the subsecond time range. Di-8-ANEPPS has been used to record action potentials (Rohr and Salzberg, 1994), and the kinetics of fura-2 are consistent with measurements in the millisecond time range (Jackson et al., 1987). The speed of acquisition will ultimately be limited by the speed of wavelength switching (limited to 20 Hz in our system), the speed of image acquisition, and by the deterioration of the signal-to-noise ratio. Because in the photon noise-limited case the signal-to-noise ratio increases proportionally with illumination intensity, an excitation bandwidth wider than the 12 nm used in this study should be used (care must be taken to limit excitation bandwidths to regions of the spectrum that do not overlap; see Fig. 1). A true simultaneous measurement of $[Ca^{2+}]$ and membrane potential could also be attempted by performing single-wavelength measurements of membrane potential with di-8-ANEPPS, and of $[Ca^{2+}]_i$ with a Ca^{2+} indicator whose emission spectrum does not overlap with the emission spectrum of di-8-ANEPPS. In fact, a preliminary report has described such a measurement implemented using a high-speed laser random-scanning microscope (Patel et al., 1995).

Presence of multiple receptors for glutamate and glutamate analogs in mouse taste buds

We stimulated taste buds with the metabotropic glutamate receptor agonist L-AP4, with the ionotropic agonist NMDA, and with L-glutamate. All of these compounds elicit responses in mouse taste cells, but there are at least two different mechanisms that can be differentiated by the direction for the change in $[Ca^{2+}]_i$. Whereas L-AP4 primarily elicited decreases in $[Ca^{2+}]_i$, NMDA elicited increases in $[Ca^{2+}]_i$. In contrast, L-glutamate elicited both increases and decreases in $[Ca^{2+}]_i$ in different cells. These observations suggest that there are multiple receptors for glutamate and glutamate analogs in mouse taste cells.

Because the taste cells were stimulated by replacement of the bath solution, our measurements do not discriminate between apically localized taste receptors for L-glutamate and neurotransmitter receptors that are presumably localized in the basolateral membrane of the taste cells. However, because taste reception results in neurotransmitter release, it is expected that excitatory L-glutamate taste receptors should elicit membrane depolarization, causing opening of voltage-gated Ca^{2+} channels and resulting in an increase in $[Ca^{2+}]_i$ and neurotransmitter release. Because we primarily observed decreases in $[Ca^{2+}]_i$ upon stimulation with L-AP4, our data suggest that the L-AP4 receptor is not the receptor mediating excitatory glutamate taste responses in mouse taste cells. In contrast, L-glutamate and NMDA elicited both cell depolarization and increases in $[Ca^{2+}]_i$, as would be expected for an excitatory glutamate taste response. This observation is consistent with a preliminary report indicating that ingestion of L-glutamate or NMDA elicits similar patterns of c-fos activation in the parabranchial nucleus in rat, whereas stimulation with L-AP4 elicits a different pattern of activation (Royer et al., 1995). Because information about taste quality may be represented by different spatial activation patterns in the parabranchial nucleus, this preliminary observation suggests that glutamate and NMDA are qualitatively indistinguishable and stimulate the same taste receptors.

In an earlier study of L-arginine taste reception in catfish (Zviman et al., 1996) we found that the taste stimulus L-arginine elicited both increases and decreases in $[Ca^{2+}]_i$ in different catfish taste cells. We postulated in that study the possibility that the decreases in $[Ca^{2+}]_i$ could be linked to inhibitory responses that could play an important role in processing of taste signals within taste buds. The observations presented in this study do not rule out a role for the L-AP4 receptor as an inhibitory taste receptor involved in glutamate taste perception in mouse. In addition, we cannot absolutely rule out the role of a the L-AP4 receptor as an excitatory taste receptor in mouse because we cannot rule out the possibility that L-AP4 caused a localized increase in $[Ca^{2+}]_i$ that was not detected by our imaging system.

SUMMARY

In summary, our results demonstrate that it is possible to perform alternate measurements of membrane potential and $[Ca^{2+}]_i$ in isolated taste buds. We find that taste cells respond to glutamate analogs known to stimulate metabotropic (L-AP4) and ionotropic (NMDA) glutamate receptors with qualitatively different changes in $[Ca^{2+}]_i$. These results indicate that taste buds possess different types of glutamate receptors. The data also suggest that the receptors responding to L-AP4, presumably metabotropic L-glutamate receptors, are not the receptors mediating excitatory glutamate taste responses. Alternate optical measurement of membrane potential and $[Ca^{2+}]_i$ is a technique that should be applicable to a variety of cell systems and should be of use in the study of intracellular $[Ca^{2+}]_i$ homeostasis in cell ensembles.

APPENDIX: DETERMINATION OF THE MAGNITUDE OF THE ERROR INTRODUCED IN $[Ca^{2+}]$ ESTIMATES BY SPILLOVER OF di-8-ANEPPS FLUORESCENCE AT ULTRAVIOLET EXCITATION WAVELENGTHS

The magnitude of the errors introduced by ultraviolet spillover of di-8-ANEPPS fluorescence in the estimates of $[Ca^{2+}]$ was estimated employing a Lotus 1-2-3 spreadsheet. Because the spillover error is expected to depend on the amount of di-8-ANEPPS relative to fura-2, the calculation was started by varying, as an independent variable, the ratio (α) of the fluorescence contributed by fura-2 at 360 nm ($F_{f2,360}$) divided by the fluorescence contributed by di-8-ANEPPS fluorescence at 440 nm ($F_{di8,440}$).

$$\alpha = F_{f2,360}/F_{di8,440}. \tag{A1}$$

In addition, the calcium concentration ($[Ca^{2+}]$) was also varied as a second independent variable.

The calculations were performed step by step as follows:

1. The fluorescence emitted by di-8-ANEPPS at 440 nm ($F_{di8,440}$) was set arbitrarily to 100, and the fluorescence emitted by fura-2 at 360 nm $F_{f2,360}$ was calculated using Eq. A1.

2. The fluorescence emitted by fura-2 at 340 nm was calculated from the calcium concentration $[Ca^{2+}]$ using Eqs. A2 and A3. Equation A2 results from rearrangement of Eq. 3.

$$R = \frac{R_{min}K_d(S_{f2}/S_{b2}) + [Ca^{2+}]R_{max}}{K_d(S_{f2}/S_{b2}) + [Ca^{2+}]}. \tag{A2}$$

$$F_{f2,340} = RF_{f2,360}. \tag{A3}$$

For our fluorescence microscopy setup the values of the parameters necessary to perform this calculation were K_d = 224 nM; R_{max} = 1.27; R_{min} = 0.44; and S_{f2}/S_{b2} = 0.98.

3. The amount of fluorescence spillover from di-8-ANEPPS at 360 ($F_{di8,360}$) and 340 nm ($F_{di8,340}$) was then calculated using the percentage spillover values given in Table 5 for 0 mV, and the measured fura-2 fluorescence ratio (R_{meas}) was calculated using Eq. 3.

4. Finally, the measured calcium concentration was calculated from R_{meas} using Eq. 3, and the measured ratio of the fluorescence excited at 360 nm divided by the fluorescence excited at 440 nm (F_{360}/F_{440}) was calculated using Eq. A4:

$$F_{360}/F_{440} = (F_{f2,360} + F_{di8,360})/F_{di8,440}. \tag{A4}$$

To estimate the percentage di-8-ANEPPS spillover error induced by a 65-mV depolarization, we performed the following series of calculations:

1. The fluorescence emitted by di-8-ANEPPS at 440 nm after depolarization was estimated to be 7.5% larger than the fluorescence value before depolarization. The 7.5% increase is consistent with a 15% change in di-8-ANEPPS fluorescence measured with a 100-mV depolarization in isolated taste buds in our microscopy setup.

2. The fluorescence contributed by di-8-ANEPPS at 340 and 360 nm after depolarization was estimated from the fluorescence of di-8-ANEPPS at 440 nm using the percentage spillover values given in Table 5.

3. The new [Ca^{2+}] estimate was then calculated as stated in steps 3 and 4 above.

We would like to thank Dr. Bernd Lindemann for suggestions and for providing us with the source code for img8 and helping us with technical questions.

This work was supported by National Institutes of Health grants DC001838 and DC00566, and by a grant from the Veterans Affairs Department to JGB.

REFERENCES

Bedlack, R. S., M.-D. Wei, and L. M. Loew. 1992. Localized membrane depolarizations and localized calcium influx during electric field-guided neurite growth. *Neuron.* 9:393–403.

Bernhardt, S. J., M. Naim, U. Zehavi, and B. Lindemann. 1996. Changes in IP_3 and cytosolic Ca^{2+} in response to sugars and non-sugar sweeteners in transduction of sweet taste in the rat. *J. Physiol. (Lond.).* 490:325–336.

Bright, G. R. 1993. Multiparameter imaging of cellular function. *In* Fluorescent and Luminescent Probes for Biological Action. W. T. Mason, editor. Academic Press, New York. 204–205.

Cagan, R. H. 1980. Recognition of taste stimuli at the initial binding interaction. *In* Biochemistry of Taste and Olfaction. R. H. Cagan and M. R. Kare, editors. Academic Press, New York. 175–203.

Chacon, E., J. M. Reece, A. Nieminen, G. Zahrebeiski, B. Herman, and J. J. Lemasters. 1994. Distribution of electrical potential, pH, free Ca^{2+}, and volume inside cultured rabbit cardiac myocytes during chemical hypoxia: a multiparameter digitized confocal microscopic study. *Biophys. J.* 66:942–952.

Chaudhari, N., C. Lamp, H. Yang, A. Porter, M. Minyard, and S. D. Roper. 1994. The molecular biology of glutamate receptors in rat taste buds. *In* Olfaction and Taste XI. K. Kurihara, N. Suzuki, and H. Ogawa, editors. Springer-Verlag, Tokyo. 382–383.

Delay, R. J., R. Taylor, and S. D. Roper. 1993. Merkel-like basal cells in *Necturus* taste buds contain serotonin. *J. Comp. Neurol.* 335:606–613.

Ewald, D. A., and S. D. Roper. 1995. Intercellular signaling in *Necturus* taste buds: chemical excitation of receptor cells elicits responses in basal cells. *J. Neurophysiol.* 67:1316–1324.

Gilbertson, T. A. 1993. The physiology of vertebrate taste reception. *Curr. Opin. Neurobiol.* 3:532–539.

Gilbertson, T. A., S. D. Roper, and S. C. Kinnamon. 1993. Proton currents through amiloride-sensitive Na^+ channels in hamster taste cells: role in sour taste transduction. *Neuron.* 10:931–942.

Grynkiewicz, G., M. Poenie, and R. Y. Tsien. 1985. A new generation of Ca^{2+} indicators with greatly improved fluorescence properties. *J. Biol. Chem.* 260:3440–3450.

Jackson, A. P., M. P. Timmermann, C. R. Bagshaw, and C. C. Ashley. 1987. The kinetics of calcium binding to fura-2 and indo-1. *FEBS Lett.* 216:35–39.

Kinnamon, J. C. 1987. Organization and innervation of taste buds. *In* Neurobiology of Taste and Smell. T. E. Finger and W. L. Silver, editors. John Wiley and Sons, New York. 277–297.

Kinnamon, S. C., and T. A. Cummings. 1992. Chemosensory transduction mechanisms in taste. *Annu. Rev. Physiol.* 54:715–731.

Kremer, S. G., W. Zeng, and K. L. Skorecki. 1992. Simultaneous fluorescence measurement of calcium and membrane potential responses to endothelin. *Am. J. Physiol.* 263:C1302–C1309.

Llinas, R., M. Sugimori, and R. B. Silver. 1992. Microdomains of high calcium concentration in a presynaptic terminal. *Science.* 256:677–679.

Loew, L. M. 1993. Potentiometric membrane dyes. *In* Fluorescent and Luminescent Probes for Biological Activity. W. T. Mason, editor. Academic Press, New York. 150–160.

Loew, L. M., R. A. Tuft, W. Carrington, and F. S. Fay. 1993. Imaging in five dimensions: time-dependent membrane potentials in individual mitochondria. *Biophys. J.* 65:2396–2407.

Martinez-Zaguilan, R., G. M. Martinez, F. Lattanzio, and R. J. Gillies. 1991. Simultaneous measurement of intracellular pH and Ca^{2+} using the fluorescence of SNARF-1 and fura-2. *Am. J. Physiol.* 260:C297–C307.

Messler, P., H. Harz, and R. Uhl. 1996. Instrumentation for multiwavelength excitation imaging. *J. Neurosci. Methods.* In press.

Monck, J. R., A. F. Oberhauser, T. J. Keating, and J. M. Fernandez. 1992. Thin-section ratiometric Ca^{2+} images obtained by optical sectioning of fura-2 loaded mast cells. *J. Cell Biol.* 116:745–759.

Montana, V., D. L. Farkas, and L. M. Loew. 1989. Dual-wavelength ratiometric fluorescence measurements of membrane potential. *Biochemistry.* 28:4536–4539.

Morris, S. J., T. B. Wiegmann, L. W. Welling, and B. M. Chronwall. 1994. Rapid simultaneous estimation of intracellular calcium and pH. *In* A Practical Guide to the Study of Calcium in Living Cells. R. Nuccitelli, editor. Academic Press, New York. 184–220.

Ninomya, Y., and M. Funakoshi. 1989. Peripheral neural basis for behavioral discrimination between glutamate and the four basic taste substances in mice. *Comp. Biochem. Physiol.* 92A:371–376.

Nuccitelli, R. 1994. A Practical Guide to the Study of Calcium in Living Cells. Academic Press, New York.

Ochsner, M., T. Fleck, and P. Waldmier. 1991. Simultaneous measurement of Ca^{2+} transients and of membrane potential depolarizations in liposomes. *Biochem. Biophys. Res. Commun.* 181:797–803.

Patel, S. S., A. Bullen, and P. Saggau. 1995. Simultaneous multi-site recording with two fluorescent probes using high-speed laser random scanning microscopy. *Soc. Neurosci. Abstr.* 21:1078.

Restrepo, D., M. M. Zviman, and N. E. Rawson. 1995. Imaging of intracellular calcium in chemosensory receptor cells. *In* Experimental Cell Biology of Taste and Olfaction. A. I. Spielman and J. G. Brand, editors. CRC Press, Boca Raton, FL. 387–398.

Reutter, K. 1971. Die Geschmackskoskospen des Zwergweleses *Amiurus nebulosus* (Lesueur). Morphologisches und histochemisches Untersuchungen. *Z. Zellforsch. Mikrosk. Anat.* 120:280–308.

Reutter, K. 1978. Taste organ in the bullhead (Teleostei). *Adv. Anat. Embryol. Cell Biol.* 55:1–98.

Reutter, K., and Witt, M. 1994. Morphology of vertebrate taste organs and their nerve supply. *In* Mechanisms of Taste Transduction. S. A. Simon and S. D. Roper, editors. CRC Press, Boca Raton, FL. 29–82.

Rohr, S., and B. M. Salzberg. 1994. Multiple site optical recording of transmembrane voltage (MSORTV) in patterned growth heart cell cultures: assessing electrical behavior, with microsecond resolution, on a cellular and subcellular scale. *Biophys. J.* 67:1301–1315.

Royer, S. M., J. C. Kinnamon, and S. D. Roper. 1995. Expression of c-FOS in the rat parabranchial nucleus following ingestion of monosodium glutamate and other tastant stimuli. *Soc. Neurosci. Abstr.* 21:1658.

Teeter, J. H. 1985. Dye coupling in catfish taste buds. *Jpn. J. Taste Smell Res.* 19:29–33.

Teeter, J. H., T. Kumazawa, J. G. Brand, D. L. Kalinoski, E. Honda, and G. Smutzer. 1992. Amino acid receptor channels in taste cells. *In* Sensory Transduction. D. P. Corey and S. D. Roper, editors. Rockefeller University Press, New York. 291–306.

Yamaguchi, S. 1967. The synergistic effect of monosodium glutamate and disodium 5′-inosinate. *J. Food Sci.* 32:473–478.

Yang, J., and S. D. Roper. 1987. Dye-coupling in taste buds in the mudpuppy, *Necturus maculosus*. *J. Neurosci.* 7:3561–3565.

Zviman, M. M., D. Restrepo, and J. H. Teeter. 1996. Single taste stimuli elicit either increases or decreases in intracellular calcium in isolated catfish taste cells. *J. Membr. Biol.* 149:81–88.